OPEN ACCESS
JOURNAL OF ADVANCED DIELECTRICS
Vol. 12, No. 5 (2022) 2250014 (10 pages)

DOI: 10.1142/S2010135X2250014X

Enhancement of electro-strain performance of $KTaO_3$ modified $0.94Bi_{0.5}Na_{0.5}TiO_3$–$0.06BaTiO_3$ ceramics

Xinran Wang, Huanghui Nie, Yan Yan and Gang Liu*
Faculty of Materials and Energy, Southwest University
Chongqing 400715, P. R. China
*liugang13@swu.edu.cn

Received 4 August 2022; Revised 18 August 2022; Accepted 23 August 2022; Published 21 October 2022

The $(1-x)(0.94Bi_{0.5}Na_{0.5}TiO_3–0.06BaTiO_3)–xKTaO_3$(BNBT–$x$KT) lead-free ferroelectric ceramics were produced using the traditional solid-state sintering technique, and the phase structure, surface morphology, electrical properties were all thoroughly examined. Every ceramic has a single perovskite structure and there is no second phase, as shown by the XRD patterns and Raman spectra. Scanning electron microscopy revealed that all samples displayed dense microstructure and cubic grain. In addition, KT encourages grain growth due to the oxygen vacancies induced by doping or volatilization of ions at high temperatures. The T_m of the ceramics decreases with increasing doping levels due to oxygen vacancies acting as dipoles upon the addition of KT, and the dielectric loss of all samples is low at ambient temperature. In comparison to the pure BNBT ceramic's bipolar strain value of 0.12%, the BNBT–2KT ceramic achieved a maximum bipolar strain of ~0.506% and unipolar strain of ~ 0.430% with the corresponding d_{33}* up to 538 pm/V under 80 kV/cm field. Performance significantly improved as a result of this. A test of the correlation between temperature and ferroelectric properties shows that the largest strain value of the BNBT–2KT ceramic occurs at ambient temperature and that the phase change from ferroelectric to relaxor is complete. Additionally, it is discovered that the BNBT–3KT ceramic can sustain a stable strain across a broad temperature range, suggesting that it has good temperature stability. The aforementioned findings demonstrate that lead-based ceramics may be replaced with BNBT–xKT ceramics.

Keywords: Lead-free; relaxor ferroelectric; ergodic; electro-strain.

1. Introduction

For a range of applications, including energy storage systems, actuators, transducer devices, and sensors,[1,2] piezoelectric ceramic materials are adaptable, playing a significant part in the building of national security systems, scientific research, industrial production, and many other disciplines that are directly tied to people's daily lives,[3–5] with $Pb(Zr_xTi_{1-x})O_3$ (PZT) being the most actively investigated and utilized materials, due to their superior electromechanical characteristics at the system's morphotropic phase boundary (MPB),[6,7] and their high Curie temperature (T_c > 300°C), which enables a wider range of working temperatures.[8] However, because of their high PbO content, which will impact the environment and human health during preparation, use, and waste disposal, several nations across the world have banned the use of PZT.[9,10] Many scholars are currently devoted to develop lead-free piezoelectric ceramics with excellent performance, among which bismuth sodium titanate (BNT) offers a lot of potential to replace lead-based ones.

BNT is a relaxor ferroelectric material with a rhombohedral structure that exhibits high maximum polarization (P_{max}), high Curie temperature (T_c), and low dielectric constant (ε_r) at ambient temperature.[11] However, pure BNT ceramics have the disadvantages of high coercive field (E_c), low strain, and high remnant polarization (P_r). According to the previous investigations, electro-strain is mainly related to three factors: lattice strain, phase transition, and domain change (including the motion of domain walls and domain switching).[12] At present, the construction of phase boundaries and the generation of polar nanoregions (PNRs) by chemical doping are ideal methods to improve strain properties.[12] $Bi_{0.5}Na_{0.5}TiO_3$–$BiFeO_3$,[13] $Bi_{0.5}Na_{0.5}TiO_3$–$SrTiO_3$,[14–16] $Bi_{0.5}Na_{0.5}$-TiO_3–$CaTiO_3$,[17] $Bi_{0.5}Na_{0.5}TiO_3$–$NaNbO_3$,[18] $Bi_{0.5}Na_{0.5}TiO_3$–$Bi_{0.5}K_{0.5}TiO_3$,[19] $Bi_{0.5}Na_{0.5}TiO_3$–$(K_{0.5}Na_{0.5})$-NbO_3,[20] $Bi_{0.5}Na_{0.5}TiO_3$–$BaTiO_3$[21] and other BNT-based solid solutions were created to improve electrical characteristics, and it was discovered that they had large field-induced strain and high permittivity.[22] The binary system consisting of rhombohedral (*R3c*) BNT and tetragonal (*P4bm*) $BaTiO_3$ (BT), referred to as BNBT, has received considerable attention among these materials because of enhanced ferroelectric and piezoelectric characteristics at the MPB around x = 0.06–0.07,[23–25] but it still has some properties that are inferior to lead-based ceramics. Researchers have doped based on BNBT to further enhance performance. Zhang *et al*.[26] combined KNN with BNBT to produce a ternary system with a

*Corresponding author.

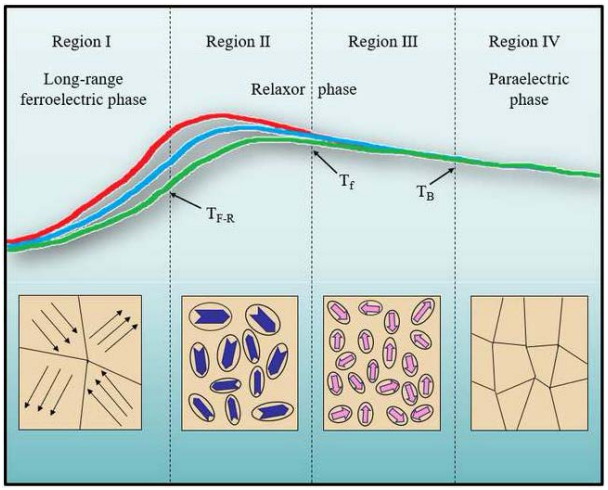

Fig. 1. Schematic diagram of phase structure of ternary system relaxor ferroelectric ceramics.

strong strain response of ~0.45 %. Li *et al*.[27] doped Nb_2O_5 into $(Bi_{0.5}Na_{0.5})_{0.94}Ba_{0.06}TiO_3$, which demonstrated a giant electro-strain of ~0.478 % under 70 kV/cm electric field at ambient temperature, while the normalized strain reached up to 654 pm/V. Wang *et al*.[28] found that under a 65 kV/cm field, the giant bipolar strain (S_{max}) was about 0.501% in their study of $(1-x)(Bi_{0.5}Na_{0.5})_{0.94}Ba_{0.06}TiO_3$–$xAgNbO_3$ ceramics.

As illustrated in Fig. 1, the doped ternary system's relaxor ferroelectric can be separated into four regions. As the temperature increases, the relaxor phase and ultimately the paraelectric phase gradually replace the long-range ordered ferroelectric phase. Below the relaxor-ferroelectric transition temperature (T_{F-R}) (Region I), there exist long-range ordered ferroelectric phases, and due to their strong interactions, they display large hysteresis and low strain responses. The strain is small due to the low dynamic characteristic of the nanodomain structure that exists between the relaxor-ferroelectric transition temperature and the relaxor temperature (T_f) (Region II). And the PNRs between the relaxor temperature and the Burns temperature (T_B), however, have smaller size, higher dynamic characteristics, and weaker correlation that can quickly react to changes in the electric field to produce low strain hysteretic and large strain (Region III).[29–32] Above the T_B, the ferroelectric properties of the ceramics disappear and turn into a paraelectric phase (Region IV).

The fundamental component chosen for this work was $0.94(Bi_{0.5}Na_{0.5})TiO_3$–$0.06BaTiO_3$, and $KTaO_3$ was modified to form ternary ceramics following the information provided above. Systematic research was done on the crystal structure, dielectric, and ferroelectric characteristics.

2. Experimental

Adopting the traditional solid-state sintering technique, a series of $(1-x)(0.94Bi_{0.5}Na_{0.5}TiO_3$–$0.06BaTiO_3)$–$xKTaO_3$ (BNBT–xKT, x = 0.01,0.02,0.03,0.04) ceramics were produced. The following substances were employed in the experiment: $BaCO_3$(99%), K_2CO_3(99%), TiO_2(99%), Na_2CO_3(99%), Bi_2O_3(99.9%), Ta_2O_5(99.99%). All medications were weighed by the stoichiometric ratio, and followed by a 24-h ball milling process in anhydrous ethanol. Then the powder was dried overnight at 70°C and was calcined for 2 h at 850°C in an air atmosphere for secondary ball milling. After drying again, 8wt% PVA was added for granulation and sieved with a 150 μm screen. Then, the discs with a diameter of 10 mm and a thickness of 1 mm were pressed on one side under 8 MPa pressure. To prevent the volatilization of ions, these prepared samples were placed in the corresponding powder and sintered for 2 h under 1120°C–1180°C. The polished and silver paste-coated sintered ceramics were then heated for 10 min at 600°C to create electrodes.

X-ray diffractometer (XRD 6100, Shimadzu, Japan) and Raman spectra (LabRAM HR Evolution, Horiba, Japan) were used to detect the crystalline structure and phase purity of the samples, and the microstructure and grain size were evaluated using a scanning electron microscope (SEM, JEOL 6610, Japan). The permittivity and dielectric loss of the sample were determined with an LCR instrument (E4980AL, Keysight, USA). Ferroelectric test equipment (TF Analyzer 2000E, aixACCT, Aachen, Germany) was used to analyze the strain curves, leakage current, and polarization hysteresis loops in a silicone oil environment.

3. Results and Discussion

Figure 2 exhibits XRD patterns and Raman spectra images of BNBT-xKT ceramics. In Fig. 2(a), the XRD patterns clearly show identical diffraction peaks for all components of the sample, indicating that the modifier KT has effectively moved into the BNBT lattice position and formed a single perovskite solid solution without a second phase. The enlarged *R3c* characteristic (111) peak at $39° < 2\theta < 41°$ and *P4bm* characteristic (200) peak at $46° < 2\theta < 47°$ were depicted in Figs. 2(b) and 2(c). It showed a single broad peak with no discernible shoulder or peak splitting, demonstrating that all ceramics had a pseudocubic structure, which is effectively a cubic non-polar phase with a fairly uniform distribution of *R3c* and *P4bm* symmetries of PNRs,[33–35] The result of the pure BNBT is consistent with several previous studies.[33–35] With increasing KT doping content, the peak slightly shifts to a lower angle of 2θ, which can be interpreted as the effect of lattice expansion caused by Ta^{5+} ions (0.64 Å) with a larger ion radius replacing Ti^{4+} (0.605 Å)[36,37] at B-site is greater than that caused by the smaller ionic radii of the K^+ ions (1.33 Å) entering A-site to replace Na^+ (1.39 Å), Bi^{3+} (1.38 Å), and Ba^{2+} (1.61 Å)[36] at the same time.[38,39]

Figure 2(d) displays the Raman spectra for BNBT-xKT ceramics, and they may be divided into four sections that correspond to the following four modes: the vibrations of the A-site cation between 100 cm^{-1} and 200 cm^{-1}, the B-site

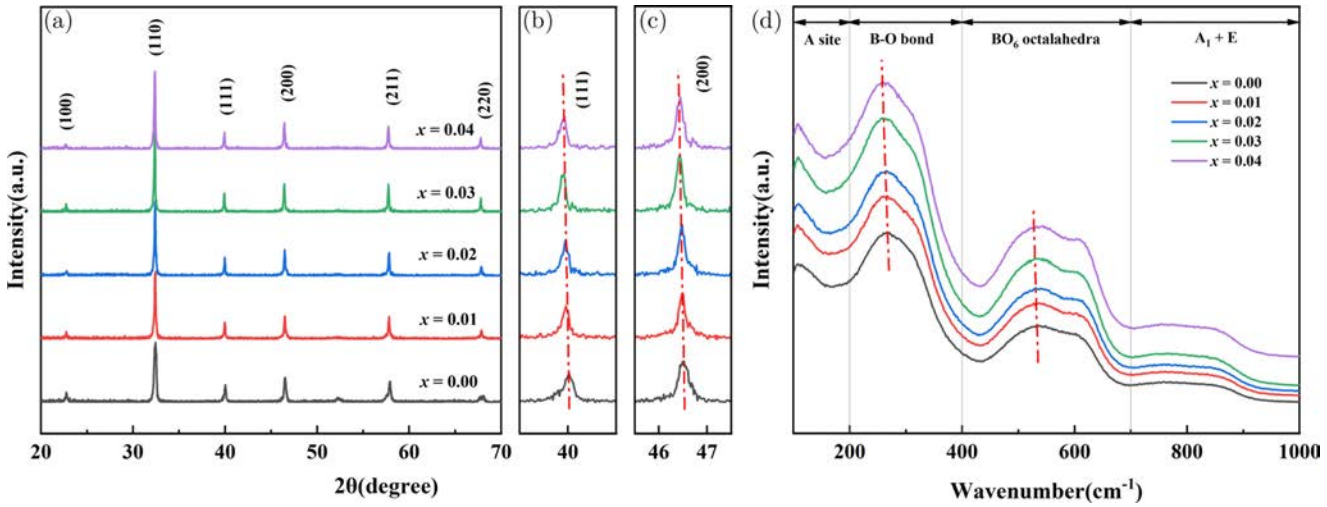

Fig. 2. XRD patterns in the 2θ range of (a) 20°–90° (b) 39°–41° (c) 45.5°–47.5° and (d) Raman spectra of BNBT–xKT ceramics.

between 200 and 400 cm^{-1},[40] the TiO_6 octahedron between 450 cm^{-1} and 750 cm^{-1},[41] as well as the overlap of A_1 (longitudinal optical) and E (longitudinal optical) above 750 cm^{-1}.[42–44] As the doping content rises, the Raman peak becomes sharper and changes to the short-wavelength direction, indicating effective diffusion of the K^+ and Ta^{5+} ions into the BNBT lattice, which alters the vibration of the A-site and B-site and raises the disorder degree of the perovskite structure.

Ceramic samples' surface and grain size are depicted in Fig. 3. As shown in Figs. 3(a)–3(e), all the samples exhibit a dense and uniform microstructure without any visible pores, and the grains reveal a cubic-type shape. Figure 3(f) demonstrates that the grain size increases as the doping level rises. This trend may be explained by the oxygen vacancies produced by acceptor doping or high-temperature volatilization of ions, two processes that are known to aid in mass transportation during the sintering process and promote grain growth.[39,45]

Figure 4 illustrates the temperature dependence for frequencies at 1 kHz, 10 kHz, 100 kHz, and 1 MHz of the dielectric constants (ε_r) and loss tangent (tanδ) of BNBT–xKT ceramics from ambient temperature up to 450°C. Images of all samples show two dielectric anomalies, T_s and T_m.

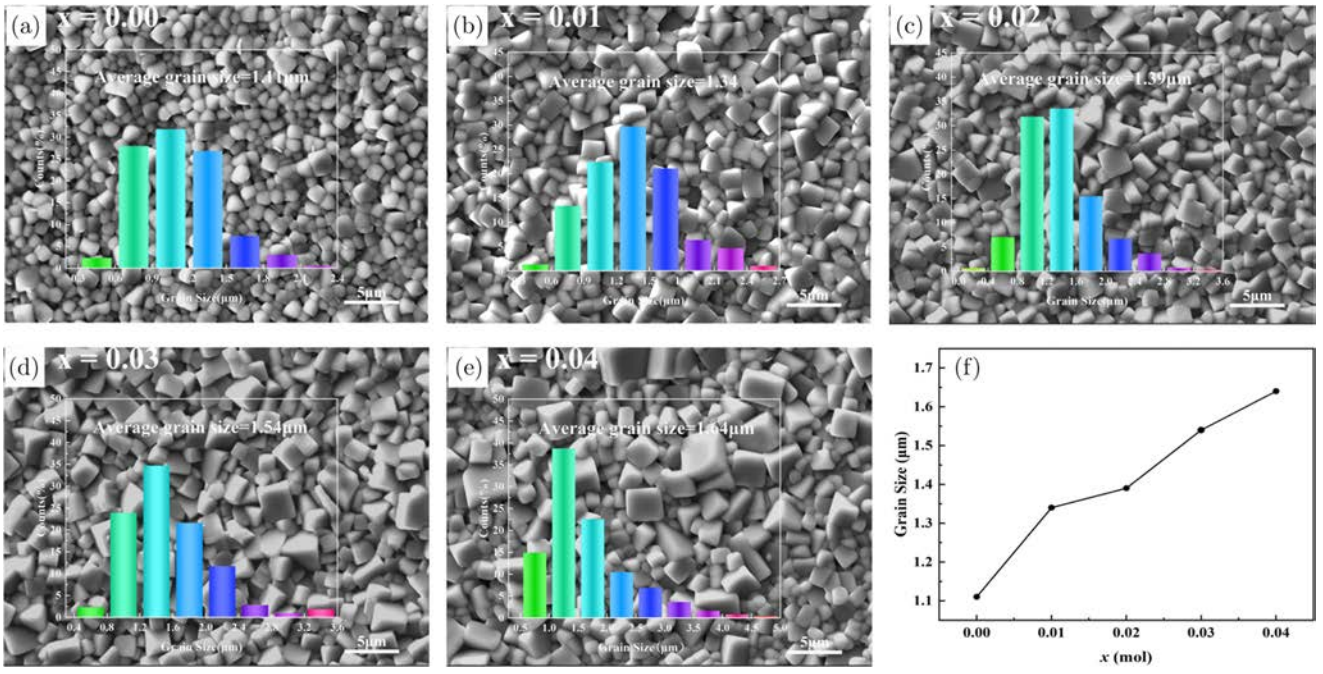

Fig. 3. (a)–(e) Scanning electron microscope images and (f) the change of grain size of BNBT–xKT samples.

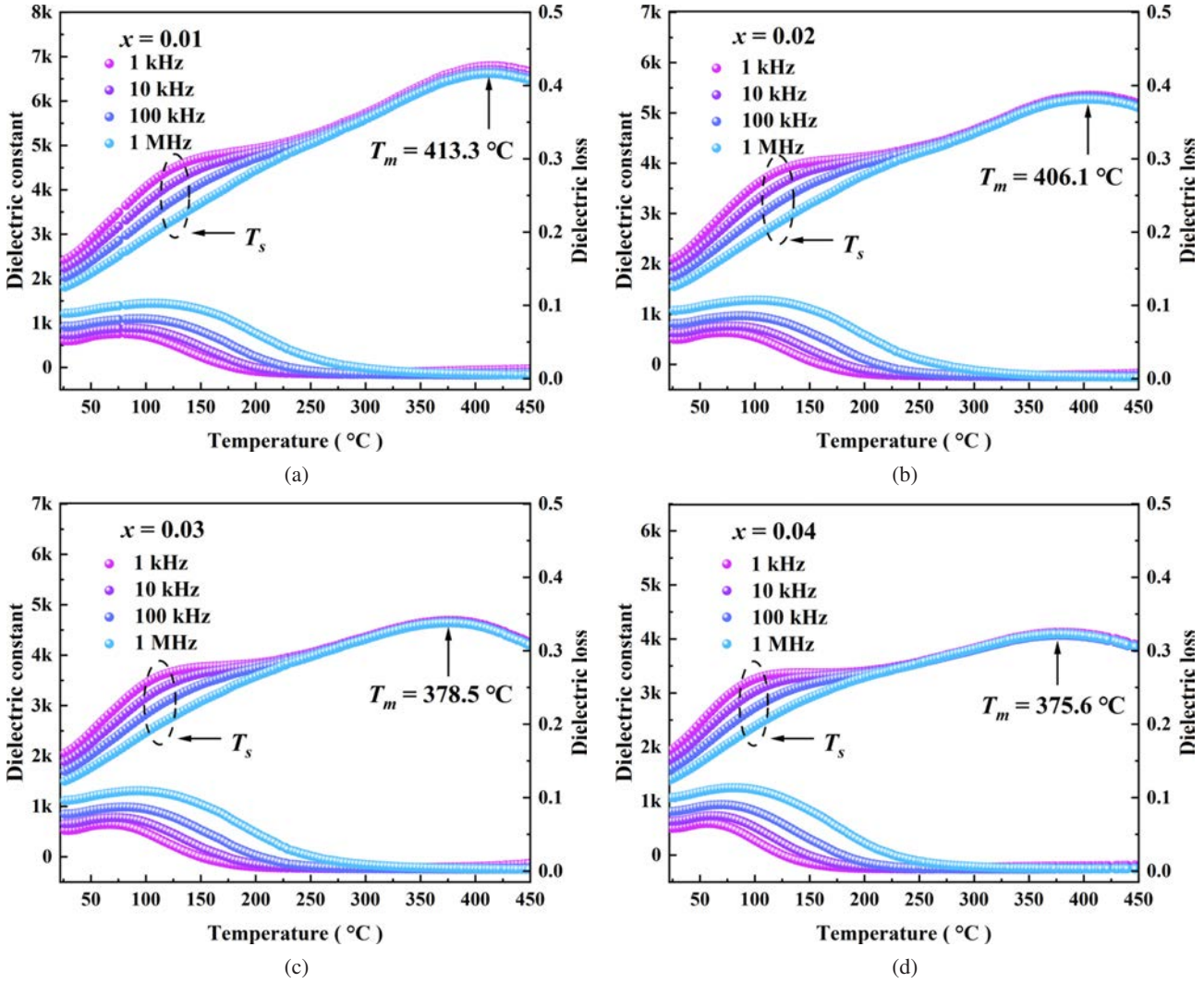

Fig. 4. Effect of temperature on loss tangent (tan δ) and dielectric constant (ε_r) for BNBT–xKT ceramics at 1 kHz, 10 kHz, 100 kHz, and 1 MHz frequency.

The first one at a lower temperature with the large frequency dispersive of T_s may be caused by the thermal activation process of PNRs,[28,46] independent of phase transition. According to theory, the size of PNRs should correlate directly with the degree of frequency dispersion.[47] The second anomaly, T_m, is the temperature that corresponds to the maximum permittivity and has no frequency dependence, suggesting the relaxor ferroelectric phase to paraelectric phase transformation is a diffuse phase transition.[11,27,48–50] Recently, it has become widely accepted that the origin of T_m results from two sequential processes that happen when the measuring temperature is raised: (1) a transition from *R3c* to *P4bm* PNRs, and (2) relaxation of these *P4bm* PNRs that are emerging from *R3c*.[39,51] T_m and T_s decrease with increasing concentration as a function, being related to the generated oxygen vacancies, which behave as defect dipoles when KT is added.[52] The phenomenon indicates KT as a modifier makes the domain transition easier and promotes the diffusion phase transition of ceramics.[53] It can be observed from Fig. 4 that all samples have a low dielectric loss.

Figure 5 demonstrates the bipolar strain (*S–E*) curves, leakage current (*J–E*) curves, and polarization hysteresis (*P–E*) loops of BNBT–xKT ceramics under an 80 kV/cm electric field. It can be seen that the pure BNBT exhibits typical ferroelectric characteristics with a saturated hysteresis loop, which is E_c of 36.37 kV/cm, P_{max} of 54.23 μc/cm^2, and P_r of 48.60 μc/cm^2. In accordance, the strain curve for BNBT has the shape of a butterfly, with a negative strain (S_{neg}) of 0.125% and a positive strain (S_{pos}) of 0.120%.

Hysteresis occurs in ferroelectric materials due to the motion of the domain walls, which is influenced by defects, such as oxygen vacancies and metal ion vacancies, which serve as pins to the domain walls.[54,55] In Figs. 5(a)–5(e), with KT's degree of doping rising, the *P-E* loops show a shrinking trend, and the waist contraction phenomenon of BNBT–0.02KT is the most obvious, both P_r and E_c decreased, which

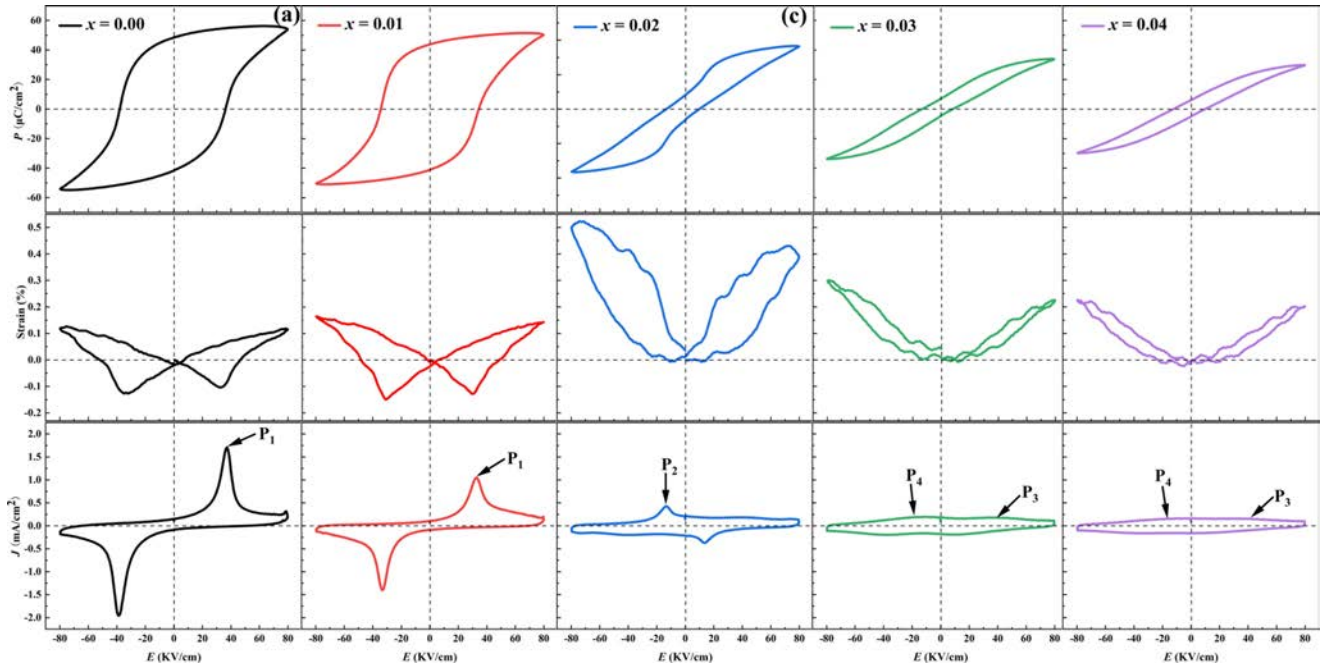

Fig. 5. The bipolar strain curves, leakage current curves, and hysteresis loops of BNBT–xKT ceramics under 80 kV/cm electric field.

is correlated with the destruction of microscopic ferroelectric structures and the formation of PNRs.[56] The relaxor behavior of samples and domain wall pinning by defects are responsible for the observed slim hysteresis loops.[55] Additionally, Fig. 5 shows that P_{max} is a function of concentration and declines as the amount of doping substance increases, indicating that the modification of KT makes the transformation of ferroelectric and relaxor ferroelectric phases irreversible. This is contrary to the change of grain size with doping content, demonstrating that the projected increase from grain expansion appears to have a smaller effect than the polarization decline that results from the major electric dipole–dipole exchange interactions.[55]

According to the switching of domains and the transformation to the relaxor phase being affected by an electric field,[57,58] the S–E curves of BNBT–xKT (x = 0.02, 0.03, 0.04) show a sprout shape rather than a butterfly shape, and the S_{neg} disappears. The positive strain initially rises and subsequently falls with the content increase, reaching the maximum strain (0.506%) at BNBT–0.02KT ceramics. The results show that the relaxor ferroelectric phase can change into long-range ordered ferroelectric domain under an applied electric field, resulting in a large strain.[59,60] The reduction in S_{pos} at x≥0.02 shows that the ferroelectric and relaxor phase transition at the same field is more difficult than it is for other compositions, due to the increase in the free energy difference.[61]

The J–E curve represents the ferroelectric domain transition.[62] A single current characteristic peak (P_1) that is indicative of the typical ferroelectric and can be attributed to the polarization inversion of the ferroelectric domain emerges at E_c in J–E curves of the pure BNBT and BNBT-1KT ceramics. In addition, the peak P_2 in the curve of BNBT–2KT is generated as ordered ferroelectric domains transit the relaxor ferroelectric phase. The peaks P_3 and P_4 are observed for BNBT–3KT and BNBT–4KT, which are related to the long-range ordered ferroelectric domain formed by disordered PNRs.[63]

The unipolar strain curves and change in d_{33}* of BNBT-xKT ceramics are depicted in Fig. 6. A linear strain effect with some hysteresis can be seen in the pure BNBT ceramic, which relates to the intrinsic piezoelectric response.[28] It can be observed that the value of strain grows initially and subsequently drops, with the increasing doping content, which changes in the same way as the unipolar strain. For BNBT-2KT ceramic, the maximum value of S is ~0.430%, and the normalized strain d_{33}* (S_{max}/E_{max})[64] is ~538 pm/V. This has to do with the ferroelectric phase and ergodic relaxor phase coexisting.[65]

Based on the analysis mentioned above, temperature's impact on the hysteresis and strain curves of BNBT–xKT (x = 0, 0.02, and 0.03) ceramics were investigated, which is depicted in Fig. 7. Moreover, Fig. 8 illustrates the change of strain value at 30°C, 50°C, 70°C, 90°C, and 110°C.

It can be observed in Figs. 7(a) and 7 (b) that the pure BNBT ceramic exhibits ferroelectricity throughout the heating process from ambient temperature to 110°C. The S–E curve changes from butterfly to sprout type, the S_{pos} increases while the E_c decreases as the temperature rises, and the P–E loop shows a shrinking trend, which can be explained by the presence of T_{F-R} during the heating process, the temperature at which the ferroelectric phase transitions to relaxor phase.[28,66,67] It demonstrates that the pure BNBT ceramic is a

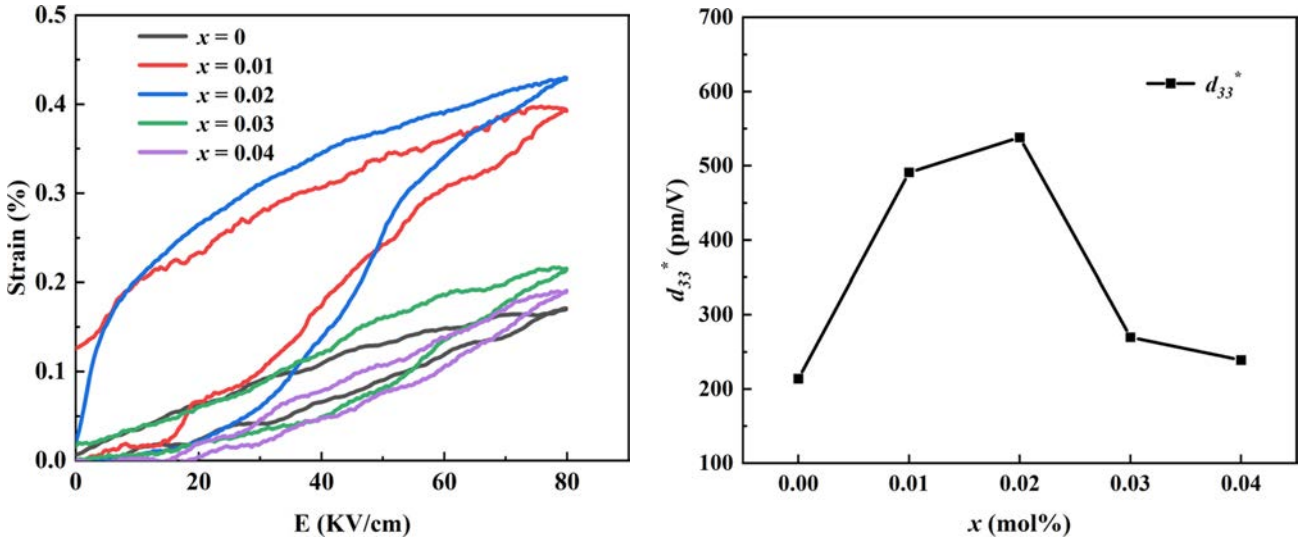

Fig. 6. (a) Unipolar strain and (b) the normalized strain d_{33}* of BNBT–xKT ceramics.

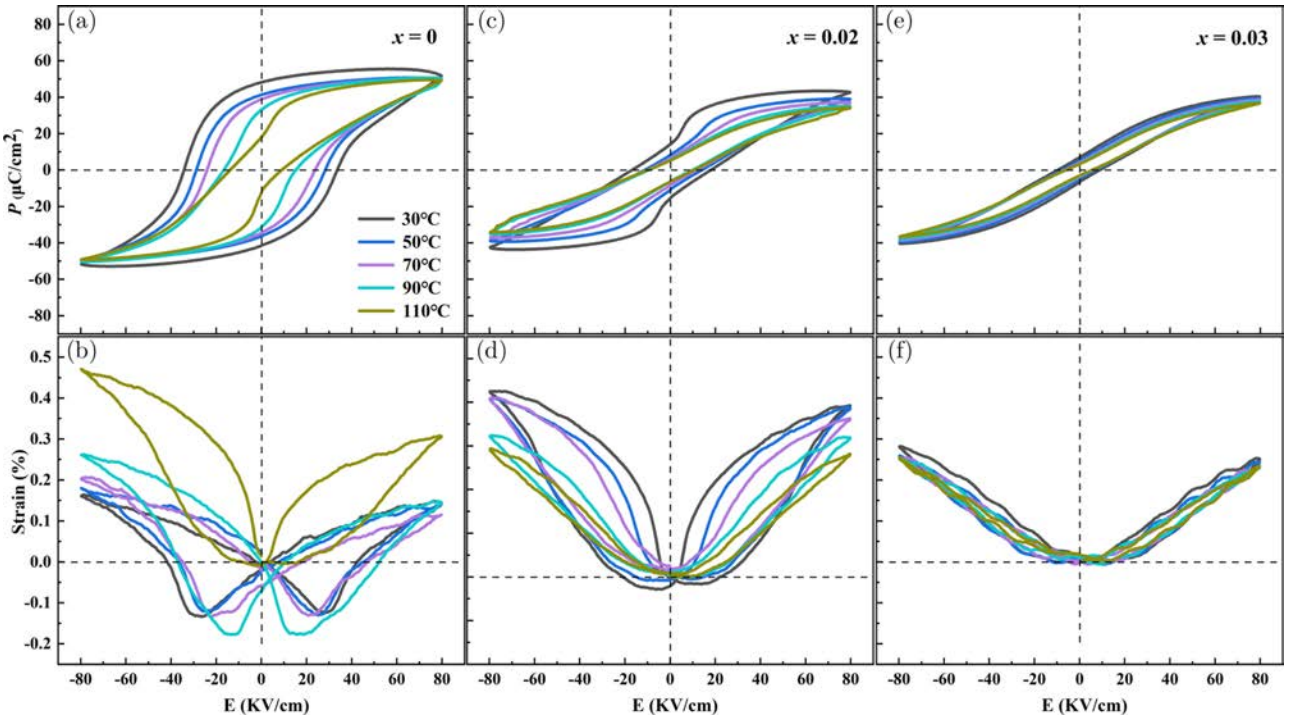

Fig. 7. Temperature's impact on the hysteresis and strain curves of (a), (b) BNBT–0KT, (c), (d) BNBT–2KT, and (e), (f) BNBT–3KT.

non-ergodic relaxor phase at room temperature.[68] Figures 7(c) and 7(d) show the characteristics of the BNBT–2KT ceramic. Since room temperature, its *S*–*E* curves show a sprout shape, and *P*–*E* curves also show obvious waist shrinkage, which indicates that the BNBT–2KT ceramic attains an ergodic relaxor state at ambient temperature.[28] The P_{max} and S_{pos} decrease with the rising temperature, while the S_{neg} almost disappears at high temperature, indicating that the large strain values always occur near the temperature of ferroelectric and relaxor phase transition. In addition, the phenomenon can be attributed to an increase in the non-polar region containing dynamic PNRs while the reduction of polar region.[69] For the BNBT–3KT ceramic, it can be seen in Figs. 7(e), 7(f) and 8 that its *P*–*E* and *S*–*E* curves are highly overlapped, and the change of strain value is less than 10%, indicating that it has a stable ergodic relaxor phase during the heating process, and displaying a steady strain response over a wide temperature range.

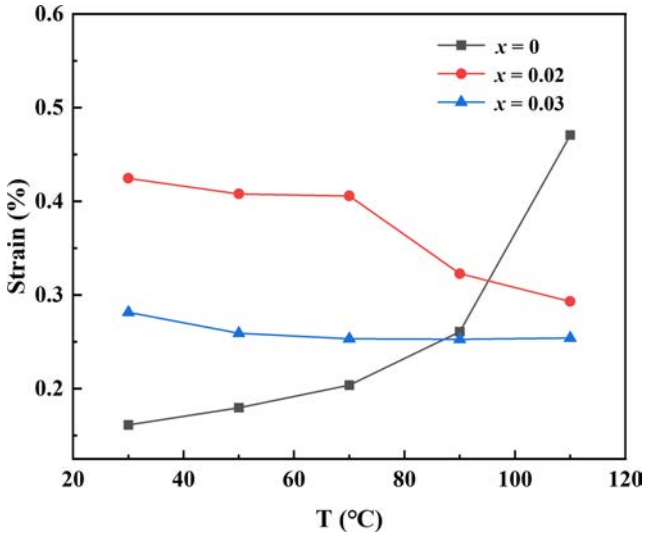

Fig. 8. The change of strain value at 30°C, 50°C, 70°C, 90°C, 110°C for BNBT–xKT (x = 0, 0.02, 0.03).

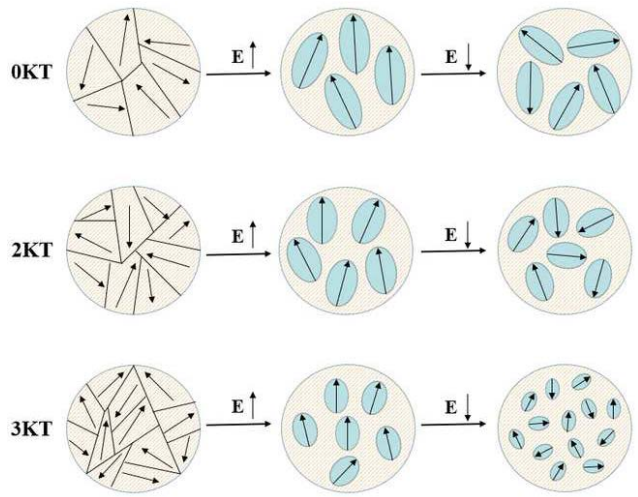

Fig. 9. Schematic illustration of the local structural changes of BNBT–xKT ceramics during polarization and depolarization processes.

Figure 9 shows the local structural changes of BNBT–xKT ceramics during polarization and depolarization processes. The pure BNBT is a non-ergodic relaxor that can make an irreversible transition to the long-range ordered ferroelectric phase under an electric field, which is field-forced polar domain growth.[35,67,70–75] Electric field influence on the local structure will be diminished by the local random field augmentation brought on by KT doping,[76,77] and the effect will get smaller as the doping content increases.[73–75] Increased ergodicity and essentially comparable free energy for the ergodic relaxor phase and non-ergodic relaxor phase characterize the BNBT–2KT ceramic. Under the influence of an applied electric field, the metastable ferroelectric structure can be established,[76–80] leading to a significant electrostrictive effect.[81–84] BNBT–2KT can quickly resume its original state after the external electric field unloads because of its intense local random field. In addition, PNRs have higher dynamic properties and smaller sizes as a result of the high substitution content of BNBT–3KT and BNBT–4KT. Hence, electric field energy is required to force the growth of domains, which further complicates local ordering and makes it more difficult to generate large strains.[81–84]

4. Conclusion

The BNBT–xKT ternary system ceramics were obtained by the traditional solid-state sintering technique. The phase structure, microstructure, and electrical characteristics of the ceramics were researched thoroughly. According to the research results, all samples have single perovskite structure, and the introduction of KT causes growth in grain size. At room temperature, the relaxor behavior of the ternary system ceramics can be observed. For the BNBT–2KT ceramic, its hysteresis loop shows an obvious waist shrinkage phenomenon, and the large bipolar strain is 0.506% while the unipolar strain and its corresponding d_{33}* are respectively 0.430% and 538 pm/V at 80 kV/cm electric field. During the heating process of 30°C–110°C, BNBT-3KT ceramic obtained highly overlapped strain curves and hysteresis loops, which indicates good thermal stability. Furthermore, the temperature dependence of strain and hysteresis demonstrates that at ambient temperature, the BNBT–2KT and BNBT–3KT ceramics establish an ergodic relaxor state. These results indicate that BNBT–xKT ceramics have better properties than pure BNBT, like low coercive field, low remnant polarization, low dielectric loss, high dielectric constant, and large electro-strain. Consequently, BNBT–xKT ceramics are an ideal replacement for lead-based ceramics and possess the potential for application in strain sensors.

Acknowledgment

The authors are grateful for the financial sponsorship of the National Natural Science Foundation of China (52073235).

References

[1]J. Koruza, A. J. Bell, T. Fromling, K. G. Webber, K. Wang and J. Rodel, Requirements for the transfer of lead-free piezoceramics into application, *J. Materiomics* **4**, 13 (2018).
[2]L. Yang, X. Kong, F. Li, H. Hao, Z. Cheng, H. Liu, J.-F. Li and S. Zhang, Perovskite lead-free dielectrics for energy storage applications, *Prog. Mater. Sci.* **102**, 72 (2019).
[3]T. Zheng, J. G. Wu, D. Q. Xiao and J. G. Zhu, Recent development in lead-free perovskite piezoelectric bulk materials, *Prog. Mater. Sci.* **98**, 552 (2018).
[4]J. G. Hao, W. Li, J. W. Zhai and H. Chen, Progress in high-strain perovskite piezoelectric ceramics, *Mater. Sci. Eng. R-Rep.* **135**, 1 (2019).
[5]G. Liu, M. Y. Tang, X. Hou, B. A. Guo, J. W. Lv, J. Dong, Y. Wang, Q. Li, K. Yu, Y. Yan and L. Jin, Energy storage properties

of bismuth ferrite based ternary relaxor ferroelectric ceramics through a viscous polymer process, *Chem. Eng. J.* **412**, 12 (2021).
[6]K. Nakamura, *Ultrasonic Transducers* (Woodhead Publishing, 2012) 70 pp.
[7]B. Jaffe, W. R. Cook and H. Jaffe, *Piezoelectric Ceramics* (Academic Press, 1971).
[8]S. J. Zhang, J. Luo, D. W. Snyder and T. R. Shrout, *Handbook of Advanced Dielectric, Piezoelectric and Ferroelectric Materials* (Woodhead Publishing, 2008) 130 pp.
[9]G. Liu, Y. Li, M. Q. Shi, L. J. Yu, P. Chen, K. Yu, Y. Yan, L. Jin, D. W. Wang and J. H. Gao, An investigation of the dielectric energy storage performance of $Bi(Mg_{2/3}Nb_{1/3})O_3$-modifed $BaTiO_3$ Pb-free bulk ceramics with improved temperature/frequency stability, *Ceram. Int.* **45**, 19189 (2019).
[10]G. Liu, Y. Li, B. Guo, M. Y. Tang, Q. Li, J. Dong, L. J. Yu, K. Yu, Y. Yan, D. W. Wang, L. Y. Zhang, H. B. Zhang, Z. B. He and L. Jin, Ultrahigh dielectric breakdown strength and excellent energy storage performance in lead-free barium titanate-based relaxor ferroelectric ceramics via a combined strategy of composition modification, viscous polymer processing, and liquid-phase sintering, *Chem. Eng. J.* **398**, 10 (2020).
[11]G. A. Smolenskii, V. A. Isupov, A. I. Agranovskaya and N. N. Krainik, New ferroelectrics of complex composition 4, *Soviet Phys.-Solid State* **2**, 2651 (1961).
[12]X. Xia, X. A. Jiang, J. T. Zeng, L. Y. Zheng, Z. Y. Man, H. R. Zeng and G. R. Li, Critical state to achieve a giant electric field-induced strain with a low hysteresis in relaxor piezoelectric ceramics, *J. Materiomics* **7**, 1143 (2021).
[13]Z. M. Tian, Y. S. Zhang, S. L. Yuan, M. S. Wu, C. H. Wang, Z. Z. Ma, S. X. Huo and H. N. Duan, Enhanced multiferroic properties and tunable magnetic behavior in multiferroic $BiFeO_3$-$Bi_{0.5}Na_{0.5}TiO_3$ solid solutions, *Mater. Sci. Eng. B-Adv. Funct. Solid-State Mater.* **177**, 74 (2012).
[14]K. Sakata and Y. Masuda, Ferroelectric and antiferroelectric properties of $(Na_{0.5}\ Bi_{0.5})TiO_3$-$SrTiO_3$ solid-solution ceramics, *Ferroelectrics* **7**, 347 (1974).
[15]G. Liu, J. Dong, L. Zhang, Y. Yan, R. Jing and L. Jin, Phase evolution in $(1-x)(Na_{0.5}Bi_{0.5})TiO_3$-$xSrTiO_3$ solid solutions: A study focusing on dielectric and ferroelectric characteristics, *J. Materiomics* **6**, 677 (2020).
[16]F. Z. Zeng, M. H. Cao, L. Zhang, M. Liu, H. Hao, Z. H. Yao and H. X. Liu, Microstructure and dielectric properties of SrTiO3 ceramics by controlled growth of silica shells on SrTiO3 nanoparticles, *Ceram. Int.* **43**, 7710 (2017).
[17]T. Takenaka, K. Sakata and K. Toda, Acoustic-wave characteristics of lead-free $(Bi_{1/2}Na_{1/2})0.99Ca0.01TiO_3$ piezoelectric ceramic, *Jpn. J. Appl. Phys. Part 1 - Regul. Pap. Short* Notes *Rev. Pap.* **28**, 59 (1989).
[18]T. Takenaka, T. Okuda and K. Takegahara, Lead-free piezoelectric ceramics based on $(Bi_{1/2}Na_{1/2})TiO_3$-$NaNbO_3$, *Ferroelectrics* **196**, 495 (1997).
[19]Z. Yang, B. Liu, L. Wei and Y. Hou, Structure and electrical properties of $(1-x)Bi_{0.5}Na_{0.5}TiO_3$–$xBi_{0.5}K_{0.5}TiO_3$ ceramics near morphotropic phase boundary, *Mater. Res. Bull.* **43**, 81 (2008).
[20]L. Gao, W. C. Zhou, F. Luo, D. M. Zhu and J. Wang, Dielectric and microwave absorption properties of KNN/Al_2O_3 composite ceramics, *Ceram. Int.* **43**, 12731 (2017).
[21]W. J. Merz, The electric and optical behavior of batio3 single-domain crystals, *Phys. Rev.* **76**, 1221 (1949).
[22]A. K. Yadav, H. Q. Fan, B. B. Yan, C. Wang, J. W. Ma, M. C. Zhang, Z. N. Du, W. J. Wang, W. Q. Dong and S. R. Wang, High strain and high energy density of lead-free $(Bi_{0.50}Na_{0.40}K_{0.10})_{0.94}Ba_{0.06}Ti_{(1-x)}(Al_{0.50}Ta_{0.50})_xO_3$ perovskite ceramics, *J. Mater. Sci.* **55**, 11137 (2020).
[23]T. Takenaka, K. Sakata and K. Toda, Piezoelectric properties of $(Bi_{1/2}Na_{1/2})TiO_3$-based ceramics, *Ferroelectrics* **106**, 375 (1990).
[24]C. Ma, H. Z. Guo, S. P. Beckman and X. L. Tan, Creation and destruction of morphotropic phase boundaries through electrical poling: A case study of lead-free $(Bi_{1/2}Na_{1/2})TiO_3$-$BaTiO_3$ piezoelectrics, *Phys. Rev. Lett.* **109**, 5 (2012).
[25]T. Takenaka, K. Maruyama and K. Sakata, $(Bi_{1/2}Na_{1/2})TiO_3$-$BaTiO_3$ system for lead-free piezoelectric ceramics, *Jpn. J. Appl. Phys. Part 1 - Regul. Pap. Short* Notes *Rev. Pap.* **30**, 2236 (1991).
[26]S. T. Zhang, A. B. Kounga, E. Aulbach, T. Granzow, W. Jo, H. J. Kleebe and J. Rodel, Lead-free piezoceramics with giant strain in the system $Bi_{0.5}Na_{0.5}TiO_3$-$BaTiO_3$-$K_{0.5}Na_{0.5}NbO_3$. I. Structure and room temperature properties, *J. Appl. Phys.* **103**, 8 (2008).
[27]Q. Li, S. Gao, L. Ning, H. Q. Fan, Z. Y. Liu and Z. Li, Giant field-induced strain in Nb_2O_5-modified $(Bi_{0.5}Na_{0.5})(0.94)Ba_{0.06}TiO_3$ lead-free ceramics, *Ceram. Int.* **43**, 5367 (2017).
[28]H. Wang, Q. Li, A. K. Yadav, Y. X. Jia, B. B. Yan, Q. F. Quan, Q. Shen, L. Lei, W. J. Wang and H. Q. Fan, Large field-induced strain with enhanced temperature-stable dielectric properties of $AgNbO_3$-modified $(Bi_{0.5}Na_{0.5})(0.94)Ba_{0.06}TiO_3$ lead-free ceramics, *Ceram. Int.* **47**, 20900 (2021).
[29]Y. L. Huang, C. L. Zhao, B. Wu and J. G. Wux, Multifunctional $BaTiO_3$-based relaxor ferroelectrics toward excellent energy storage performance and electrostrictive strain benefiting from crossover region, *ACS Appl. Mater. Interfaces* **12**, 23885 (2020).
[30]F. Li, S. J. Zhang, D. Damjanovic, L. Q. Chen and T. R. Shrout, Local structural heterogeneity and electromechanical responses of ferroelectrics: Learning from relaxor ferroelectrics, *Adv. Funct. Mater.* **28**, 21 (2018).
[31]V. V. Shvartsman and D. C. Lupascu, Lead-free relaxor ferroelectrics, *J. Am. Ceram. Soc.* **95**, 1 (2012).
[32]C. L. Zhao, B. Wu, K. Wang, J. F. Li, D. Q. Xiao, J. G. Zhu and J. G. Wu, Practical high strain with superior temperature stability in lead-free piezoceramics through domain engineering, *J. Mater. Chem. A* **6**, 23736 (2018).
[33]H. Simons, J. Daniels, W. Jo, R. Dittmer, A. Studer, M. Avdeev, J. Rodel and M. Hoffman, Electric-field-induced strain mechanisms in lead-free $94\%(Bi_{1/2}Na_{1/2})TiO_3$-$6\%BaTiO_3$, *Appl. Phys. Lett.* **98**, 3 (2011).
[34]J. E. Daniels, W. Jo, J. Rodel and J. L. Jones, Electric-field-induced phase transformation at a lead-free morphotropic phase boundary: Case study in a $93\%(Bi_{0.5}Na_{0.5})TiO_3$-$7\%$ $BaTiO_3$ piezoelectric ceramic, *Appl. Phys. Lett.* **95**, 3 (2009).
[35]W. Jo, S. Schaab, E. Sapper, L. A. Schmitt, H. J. Kleebe, A. J. Bell and J. Rodel, On the phase identity and its thermal evolution of lead free $(Bi_{1/2}Na_{1/2})TiO_3$-6 mol% $BaTiO_3$, *J. Appl. Phys.* **110**, 9 (2011).
[36]R. D. Shannon, revised effective ionic-radii and systematic studies of interatomic distances in halides and chalcogenides, *Acta Crystallogr. Sect. A* **32**, 751 (1976).
[37]J. G. Hao, Z. J. Xu, R. Q. Chu, W. Li, P. Fu, J. Du and G. R. Li, Structure evolution and electrostrictive properties in $(Bi_{0.5}Na_{0.5})(0.94)Ba_{0.06}TiO_3$-$M_2O_5$ (M = Nb, Ta, Sb) lead-free piezoceramics, *J. Eur. Ceram. Soc.* **36**, 4003 (2016).
[38]Y. Hiruma, K. Yoshii, H. Nagata and T. Takenaka, Phase transition temperature and electrical properties of $(Bi_{(1/2)}Na_{(1/2)})TiO_{(3)}$-$(Bi_{(1/2)}A_{(1/2)})TiO_{(3)}$ (A=Li and K) lead-free ferroelectric ceramics, *J. Appl. Phys.* **103**, 7 (2008).
[39]S. Prasertpalichat, S. Khengkhatkan, T. Siritanon, J. Jutimoosik, P. Kidkhunthod, T. Bongkarn and E. A. Patterson, Comparison of structural, ferroelectric, and piezoelectric properties between A-site and B-site acceptor doped $0.93Bi_{0.5}Na_{0.5}TiO_3$-$0.07BaTiO_3$ lead-free piezoceramics, *J. Eur. Ceram. Soc.* **41**, 4116 (2021).
[40]Q. Li, C. Wang, W. M. Zhang and H. Q. Fan, Influence of compositional ratio K/Na on structure and piezoelectric properties in $(Na_{1-x}K_x)_{(0.5)}Bi_{0.5}\ Ti_{0.985}Ta_{0.015}O_3$ ceramics, *J. Mater. Sci.* **54**, 4523 (2019).

[41]J. N. Sui, H. Q. Fan, H. J. Peng, J. W. Ma, A. K. Yadav, W. Chao, M. C. Zhang and G. Z. Dong, Enhanced energy-storage performance and temperature-stable dielectric properties of (1-x) $(Na_{0.5}Bi_{0.5})$ $(0.95)Ba_{0.05}$ $(0.98)La_{0.02}TiO_3$-$xK_{(0.5)}Na_{(0.5)}NbO_{(3)}$ lead-free ceramics, *Ceram. Int.* **45**, 20427 (2019).

[42]S. Manotham, P. Butnoi, P. Jaita, N. Kumar, K. Chokethawai, G. Rujijanagul and D. P. Cann, Large electric field-induced strain and large improvement in energy density of bismuth sodium potassium titanate-based piezoelectric ceramics, *J. Alloy. Compd.* **739**, 457 (2018).

[43]E. Aksel, J. S. Forrester, B. Kowalski, M. Deluca, D. Damjanovic and J. L. Jones, Structure and properties of Fe-modified $Na_{0.5}Bi_{0.5}TiO_3$ at ambient and elevated temperature, *Phys. Rev. B* **85**, 11 (2012).

[44]S. Praharaj and D. Rout, Estimation of relaxor behavior in Sr2+ doped $Na_{0.5}Bi_{0.5}TiO_3$ ceramics, *J. Mater. Sci.-Mater. Electron.* **31**, 5554 (2020).

[45]E. Taghaddos, M. Hejazi and A. Safari, Electromechanical Properties of Acceptor-Doped Lead-Free Piezoelectric Ceramics, *J. Am. Ceram. Soc.* **97**, 1756 (2014).

[46]A. Singh and R. Chatterjee, 0.40% Bipolar Strain in Lead Free BNT-KNN System Modified with Li, Ta and Sb, *J. Am. Ceram. Soc.* **96**, 509 (2013).

[47]P. Yadav, S. Sharma and N. P. Lalla, Coexistence of domain relaxation with ferroelectric phase transitions in $BaTiO_3$, *J. Appl. Phys.* **121**, 9 (2017).

[48]C. R. Zhou and X. Y. Liu, Dielectric and piezoelectric properties of $Bi_{0.5}Na_{0.5}TiO_3$-$BaNb_2O_6$ lead-free piezoelectric ceramics, *J. Mater. Sci.-Mater. Electron.* **19**, 29 (2008).

[49]A. Ullah, C. W. Ahn, A. Hussain and I. W. Kim, The effects of sintering temperatures on dielectric, ferroelectric and electric field-induced strain of lead-free $Bi_{0.5}(Na_{0.78}K_{0.22})(0.5)TiO_3$ piezoelectric ceramics synthesized by the sol-gel technique, *Curr. Appl. Phys.* **10**, 1367 (2010).

[50]C. Xu, D. Lin and K. W. Kwok, Structure, electrical properties and depolarization temperature of $(Bi_{0.5}Na_{0.5})TiO_3$–$BaTiO_3$ lead-free piezoelectric ceramics, *Solid State Sciences* **10**, 934 (2008).

[51]W. Jo, R. Dittmer, M. Acosta, J. D. Zang, C. Groh, E. Sapper, K. Wang and J. Rodel, Giant electric-field-induced strains in lead-free ceramics for actuator applications - status and perspective, *J. Electroceram.* **29**, 71 (2012).

[52]C. H. Lee, H. S. Han, T. A. Duong, T. H. Dinh, C. W. Ahn and J. S. Lee, Stabilization of the relaxor phase by adding CuO in lead-free $(Bi_{1/2}Na_{1/2})$ TiO_3-$SrTiO_3$-$BiFeO_3$ ceramics, *Ceram. Int.* **43**, 11071 (2017).

[53]A. Hussain, J. U. Rahman, A. Zaman, R. A. Malik, J. S. Kim, T. K. Song, W. J. Kim and M. H. Kim, Field-induced strain and polarization response in lead-free $Bi_{1/2}(Na_{0.80}K_{0.20})(1/2)TiO_3$-$SrZrO_3$ ceramics, *Mater. Chem. Phys.* **143**, 1282 (2014).

[54]K. S. Rao, D. M. Prasad, P. M. Krishna, T. S. Latha and J. H. Lee, Electrical and electromechanical studies on tungsten-bronze electroceramic: Lead potassium dysprosium niobate, *Optoelectron. Adv. Mater.-Rapid Commun.* **1**, 510 (2007).

[55]S. Anem, K. S. Rao and K. H. Rao, Investigation of lanthanum substitution in lead-free BNBT ceramics for transducer applications, *Ceram. Int.* **42**, 15319 (2016).

[56]Y. C. Wu, G. S. Wang, Z. Jiao and X. L. Dong, Excellent temperature stability with giant electrostrain in Bi0.5Na0.5TiO3-based ceramics, *Scr. Mater.* **179**, 70 (2020).

[57]G. Z. Dong, H. Q. Fan, Y. X. Jia, H. Liu, W. J. Wang and Q. Li, Strain properties of $(1-x)Bi_{0.5}Na_{0.4}K_{0.1}TiO_3$-$xBi(Mg_{2/3}Ta_{1/3})O_3$ electroceramics, *Ceram. Int.* **46**, 21211 (2020).

[58]Q. Li, L. Ning, B. Hu, H. J. Peng, N. S. Zhao and H. Q. Fan, Large strain response in $(1-x)(0.94Bi_{(0.5)}Na_{(0.5)}TiO_{(3)}$-$0.06BaTiO_{(3)})$ $xSr_{(0.8)}Bi_{(0.1)}$square $0.1Ti_{0.8}Zr_{0.2}O_{2.95}$ lead-free piezoelectric ceramics, *Ceram. Int.* **45**, 1676 (2019).

[59]J. H. Han, J. Yin and J. G. Wu, BNT-based ferroelectric ceramics: Electrical properties modification by Ta_2O_5 oxide addition, *J. Am. Ceram. Soc.* **103**, 412 (2020).

[60]H. Y. He, W. H. Lu, J. A. S. Oh, Z. R. Li, X. Lu, K. Y. Zeng and L. Lu, Probing the coexistence of ferroelectric and relaxor states in $Bi_{0.5}Na_{0.5}TiO_3$-based ceramics for enhanced piezoelectric performance, *ACS Appl. Mater. Interfaces* **12**, 30548 (2020).

[61]T. Li, X. J. Lou, X. Q. Ke, S. D. Cheng, S. B. Mi, X. J. Wang, J. Shi, X. Liu, G. Z. Dong, H. Q. Fan, Y. Z. Wang and X. L. Tan, Giant strain with low hysteresis in A-site-deficient $(Bi_{0.5}Na_{0.5})$ TiO_3-based lead-free piezoceramics, *Acta Mater.* **128**, 337 (2017).

[62]J. G. Hao, B. Shen, J. W. Zhai, C. Z. Liu, X. L. Li and X. Y. Gao, Switching of morphotropic phase boundary and large strain response in lead-free ternary $(Bi_{0.5}Na_{0.5})TiO_3$-$(K_{0.5}Bi_{0.5})TiO_3$-$(K_{0.5}Na_{0.5})NbO_3$ system, *J. Appl. Phys.* **113**, 13 (2013).

[63]H. Wang, Q. Li, Y. X. Jia, A. K. Yadav, B. B. Yan, M. Y. Li, Q. F. Quan, W. J. Wang and H. Q. Fan, Large electro-strain with excellent fatigue resistance of lead-free $(Bi_{0.5}Na_{0.5})(0.94)Ba_{0.06}Ti_{1-x}(Y_{0.5}Nb_{0.5})(x)O_3$ perovskite ceramics, *Ceram. Int.* **47**, 17092 (2021).

[64]Y. M. Li, W. Chen, Q. Xu, J. Zhou and X. Y. Gu, Piezoelectric and ferroelectric properties of $Na_{0.5}Bi_{0.5}TiO_3$-$K_{0.5}Bi_{0.5}TiO_3$-$BaTiO_3$ piezoelectric ceramics, *Mater. Lett.* **59**, 1361 (2005).

[65]E. Sapper, N. Novak, W. Jo, T. Granzow and J. Rodel, Electric-field-temperature phase diagram of the ferroelectric relaxor system $(1-x)Bi_{1/2}Na_{1/2}TiO_3$-$xBaTiO_{(3)}$ doped with manganese, *J. Appl. Phys.* **115**, 7 (2014).

[66]W. F. Bai, D. Q. Chen, Y. W. Huang, B. Shen, J. W. Zhai and Z. G. Ji, Electromechanical properties and structure evolution in $BiAlO_3$-modified $Bi_{0.5}Na_{0.5}TiO_3$-$BaTiO_3$ lead-free piezoceramics, *J. Alloy. Compd.* **667**, 6 (2016).

[67]W. Jo, T. Granzow, E. Aulbach, J. Rodel and D. Damjanovic, Origin of the large strain response in $(K_{0.5}Na_{0.5})NbO_3$-modified $(Bi_{0.5}Na_{0.5})TiO_3$-$BaTiO_3$ lead-free piezoceramics, *J. Appl. Phys.* **105**, 5 (2009).

[68]W. F. Bai, D. Q. Chen, Y. W. Huang, P. Zheng, J. S. Zhong, M. Y. Ding, Y. J. Yuan, B. Shen, J. W. Zhai and Z. G. Ji, Temperature-insensitive large strain response with a low hysteresis behavior in BNT-based ceramics, *Ceram. Int.* **42**, 7669 (2016).

[69]J. Shi, X. Liu and W. C. Tian, High energy-storage properties of $Bi_{0.5}Na_{0.5}TiO_3$-$BaTiO_3$-$SrTi_{0.875}Nb_{0.1}O_3$ lead-free relaxor ferroelectrics, *J. Mater. Sci. Technol.* **34**, 2371 (2018).

[70]W. Jo and J. Rodel, Electric-field-induced volume change and room temperature phase stability of $(Bi_{1/2}Na_{1/2})TiO_3$-x mol. % BaTiO3 piezoceramics, *Appl. Phys. Lett.* **99**, 3 (2011).

[71]J. G. Hao, B. Shen, J. W. Zhai and H. Chen, Phase transitional behavior and electric field-induced large strain in alkali niobate-modified $Bi_{0.5}(Na_{0.80}K_{0.20})(0.5)TiO_3$ lead-free piezoceramics, *J. Appl. Phys.* **115**, 8 (2014).

[72]W. F. Bai, L. Y. Li, W. Li, B. Shen, J. W. Zhai and H. Chen, Phase Diagrams and Electromechanical Strains in Lead-Free BNT-Based Ternary Perovskite Compounds, *J. Am. Ceram. Soc.* **97**, 3510 (2014).

[73]Q. R. Yao, F. F. Wang, F. Xu, C. M. Leung, T. Wang, Y. X. Tang, X. Ye, Y. Q. Xie, D. Sun and W. Z. Shi, Electric Field-Induced Giant Strain and Photoluminescence-Enhancement Effect in Rare-Earth Modified Lead-Free Piezoelectric Ceramics, *ACS Appl. Mater. Interfaces* **7**, 5066 (2015).

[74]D. Liu, C. Y. Tian, C. G. Ma, L. H. Luo, Y. X. Tang, T. Wang, W. Z. Shi, D. Z. Sun and F. F. Wang, Composition, electric-field and temperature induced domain evolution in lead-free $Si_{0.5}Na_{0.5}TiO_3$-$BaTiO_3$-$SrTiO_3$ solid solutions by piezoresponse force microscopy, *Scr. Mater.* **123**, 64 (2016).

[75]R. Dittmer, W. Jo, J. Rodel, S. Kalinin and N. Balke, Nanoscale insight into lead-free BNT-BT-xKNN, *Adv. Funct. Mater.* **22**, 4208 (2012).

[76]V. Westphal, W. Kleemann and M. D. Glinchuk, Diffuse phase-transitions and random-field-induced domain states of the relaxor ferroelectric $PbMg_{1/3}Nb_{2/3}O_3$, *Phys. Rev. Lett.* **68**, 847 (1992).
[77]F. Li, D. B. Lin, Z. B. Chen, Z. X. Cheng, J. L. Wang, C. C. Li, Z. Xu, Q. W. Huang, X. Z. Liao, L. Q. Chen, T. R. Shrout and S. J. Zhang, Ultrahigh piezoelectricity in ferroelectric ceramics by design, *Nat. Mater.* **17**, 349 (2018).
[78]D. W. Zhang, Y. G. Yao, M. X. Fang, Z. D. Luo, L. X. Zhang, L. L. Li, J. Cui, Z. J. Zhou, J. H. Bian, X. B. Ren and Y. D. Yang, Isothermal phase transition and the transition temperature limitation in the lead-free (1-x)$Bi_{0.5}Na_{0.5}TiO_3$-x$BaTiO_{(3)}$ system, *Acta Mater.* **103**, 746 (2016).
[79]F. Li, G. R. Chen, X. Liu, J. W. Zhai, B. Shen, S. D. Li, P. Li, K. Yang, H. R. Zeng and H. X. Yan, Type-I pseudo-first-order phase transition induced electrocaloric effect in lead-free $Bi_{0.5}Na_{0.5}TiO_3$-0.06$BaTiO_{(3)}$ ceramics, *Appl. Phys. Lett.* **110**, 5 (2017).
[80]D. Wang, X. Q. Ke, Y. Z. Wang, J. H. Gao, Y. Wang, L. X. Zhang, S. Yang and X. B. Ren, Phase diagram of polar states in doped ferroelectric systems, *Phys. Rev. B* **86**, 7 (2012).
[81]F. Li, L. Jin, Z. Xu and S. J. Zhang, Electrostrictive effect in ferroelectrics: An alternative approach to improve piezoelectricity, *Appl. Phys. Rev.* **1**, 21 (2014).
[82]R. Pirc, R. Blinc and V. S. Vikhnin, Effect of polar nanoregions on giant electrostriction and piezoelectricity in relaxor ferroelectrics, *Phys. Rev. B* **69**, 4 (2004).
[83]F. Li, Z. Xu and S. J. Zhang, The effect of polar nanoregions on electromechanical properties of relaxor-$PbTiO_3$ crystals: Extracting from electric-field-induced polarization and strain behaviors, *Appl. Phys. Lett.* **105**, 5 (2014).
[84]X. Liu, F. Li, J. W. Zhai, B. Shen, P. Li, Y. Zhang and B. H. Liu, Enhanced electrostrictive effects in nonstoichiometric $0.99Bi_{(0.505)}(Na_{0.8}K_{0.2})$(0.5-x)$TiO_3-0.01SrTiO_{(3)}$ lead-free ceramics, *Mater. Res. Bull.* **97**, 215 (2018).